Electronic Supplementary Material (ESI) for Physical Chemistry Chemical Physics


## SUPPORTING INFORMATION

# Structural controls on OH site availability and reactivity at iron oxyhydroxide particle surfaces

Xiaowei Song and Jean-François Boily*

Department of Chemistry

Umeå University

SE-901 87 Umeå

Sweden

* corresponding author: +46 (0)90 786 5270, jean-francois.boily@chem.umu.se

### Description of force field model and parameters

Potential energy was calculated as the sum of non-bonded (Coulombic and van der Waals) and bonded (bond stretch and bend) interactions. Coulombic energy is expressed as:

$$V_C(r_{ij}) = \frac{q_i \cdot q_i}{f \cdot r_{ij}} \qquad [1]$$

where $f=4\pi\varepsilon_o\varepsilon_p e^{-2}$, $\varepsilon_o$ is the permittivity of vacuum, $\varepsilon_o$ the relative dielectric constant and $e$ elementary charge. Van der Waals energy is represented by the Lennard-Jones (12-6) function:

$$V_{LJ}(r_{ij}) = 4\varepsilon_{ij}\left(\left(\frac{\sigma_{ij}}{r_{ij}}\right)^{12} - \left(\frac{\sigma_{ij}}{r_{ij}}\right)^{6}\right) \qquad [2]$$

using Lorentz-Berthelot mixing rules:

$$\sigma_{ij} = \frac{1}{2}(\sigma_{ii} + \sigma_{jj}) \qquad [3]$$

$$\varepsilon_{ij} = \sqrt{\varepsilon_{ii}\varepsilon_{jj}} \qquad [4]$$

Finally the bonded potential energies were described by harmonic stretches

$$V_b(r_{ij}) = \frac{1}{2} k^b_{ij} (r_{ij} - b_{ij})^2 \qquad [5]$$

for all hydroxyls (O-H), and harmonic bends

$$V_a(\theta_{ijk}) = \frac{1}{2} k^\theta_{ijk} (\theta_{ijk} - \theta_{ijk})^2 \qquad [6]$$

in water (H-O-H) and bulk Fe-O-H. All modeling parameters re reported in Table 4.

**References**

1 Cygan, R. T.; Liang, J. J.; Kalinichev, A. G. *J. Phys. Chem. B* **2004,** *108* (4), 1255-1266.

2 Kerisit, S. *Geochim. Cosmochim. Ac.* **2011,** *75* (8), 2043-2061.

3 Berendsen, H. J. C.; Grigera, J. R.; Straatsma, T. P. *J. Phys. Chem.* **1987,** *91* (24), 6269-6271.)

4 Berendsen, H. J. C.; Postma, J. P. M.; Gunsterenand, W. F.; Hermans, J., In *Intermolecular Forces*, Pullman, B., Ed. D. Riedel Publishing Company: Dordrecht, The Netherlands, 1981; pp 331-342.

5 H. Yang, R. Lu, R. T. Downs and G. Costin, *Acta Crystallog. E*, 2006, **62**, i250-i252.

6 Wyckoff, R. W. G, *Crystal Structures 1*, Interscience Publishers: New York, 1963; pp 290-295.

# TABLES

**Table S1** Effects of protonation on surface OH stretching of LL

| Spectra | Hads (protons/nm$^2$) | Bands (cm$^{-1}$) | | | | |
|---|---|---|---|---|---|---|
| | | ⬩ α | ○ | ☽ | ☾ | ⚢ |
| | | 3667 | 3625 | 3552 | 3534 | 3645 |
| Aa | -13.86 | ●ß | ● | ● | ● | |
| Ab | -2.59 | ↓ | - | - | - | |
| Ac | 0.00 | ↓ | - | - | - | |
| Ad | 2.29 | ↓ | - | - | - | ● |
| Ae | 18.17 | ⊥ | ↓ | - | - | ↑ |
| Af | 36.11 | | ↓ | - | - | - |
| Ag | 53.15 | | ↓ | - | - | - |
| Ah | 143.23 | | ↓ | - | - | - |
| Ai | 312.99 | | ↓ | - | - | - |

α. Numbers in circles are the label numbers in Fig. 3-a.
ß. Behavior of bands expressed as:
●: Present in (Aa) or appeared; ⊥: Disappeared; -: Unchanged relative to previous spectrum
↑: Increased relative to previous spectrum; ↓: Decreased relative to previous spectrum

**Table S2** Effects of protonation on surface OH stretching of RL

| Spectra | Hads (protons/nm$^2$) | Bands (cm$^{-1}$) | | | | | |
|---|---|---|---|---|---|---|---|
| | | ⬩ α | ○ | ☽ | ☾ | ⬢ | ⬢ |
| | | 366 | 3626 | 3550 | 3534 | 3654 | 3646 |
| Ba | -7.85 | ●ß | ● | ● | ● | | |
| Bb | -4.59 | ↓ | - | - | - | | |
| Bc | -0.48 | ↓ | - | - | - | | |
| Bd | 0.00 | ↓ | - | - | - | | |
| Be | 0.24 | ↓ | - | - | - | | |
| Bf | 2.23 | ↓ | - | - | - | ● | |
| Bg | 4.59 | ↓ | - | - | - | ↓ | |
| Bh | 9.10 | ↓ | - | - | - | ↓ | |
| Bi | 17.82 | ↓ | ↓ | - | - | ↓ | |
| Bj | 26.08 | ↓ | ↓ | - | - | ↓ | |
| Bk | 35.67 | ⊥ | ↓ | - | - | ↓ | |
| Bl | 69.44 | | ↓ | - | - | ⊥ | ● |
| Bm | 141.13 | | ↓ | - | - | | ↓ |

α. Numbers in circles are the label numbers in Fig. 3-b.
ß. Behavior of bands expressed as:
●: Present in (Ba) or appeared; ⊥: Disappeared; -: Unchanged relative to previous spectrum
↑: Increased relative to previous spectrum; ↓: Decreased relative to previous spectrum

**Table S3** Effects of protonation on surface OH stretching of G

| Spectra | Hads (protons/nm$^2$) | Bands (cm$^{-1}$) | | | | | |
|---|---|---|---|---|---|---|---|
| | | • α | ○ | ☽ | ☾ | ₵ | † |
| | | 3661 | 3648 | 3491 | 3545 | 3576 | 3585 |
| Ca | -12.00 | ●ß | ● | ● | | | |
| Cb | -3.35 | ↓ | - | ↓ | | | |
| Cc | -1.18 | ↓ | - | ↓ | | | |
| Cd | 0.00 | ↓ | - | ↓ | | | |
| Ce | 0.48 | ↓ | - | ↓ | | | |
| Cf | 1.18 | 3658 | - | ↓ | ● | | |
| Cg | 3.00 | ↓ | - | ⊥ | ↑ | | |
| Ch | 6.18 | ↓ | - | | - | ● | |
| Ci | 9.11 | ↓ | - | | ↓ | ↑ | |
| Cj | 12.18 | ↓ | - | | ↓ | ↑ | |
| Ck | 15.03 | ↓ | - | | ↓ | ↓ | |
| Cl | 17.88 | ⊥ | ↓ | | ⊥ | ↓ | ● |
| Cm | 20.46 | | ↓ | | | ⊥ | ↓ |
| Cn | 30.90 | | ↓ | | | | ↓ |
| Co | 102.80 | | ↓ | | | | ⊥ |
| Cp | 217.04 | | ↓ | | | | |

α. Numbers in circles are the label numbers in Fig. 3-c.
ß. Behavior of bands expressed as:
●: Present in (Ca) or appeared; ⊥: Disappeared; -: Unchanged relative to previous spectrum
↑: Increased relative to previous spectrum; ↓: Decreased relative to previous spectrum

**Table S4** Potential parameters for molecular dynamics [α]

| Atom [α] | Description | q | σ | ε | Source |
|---|---|---|---|---|---|
| H | $H_2O$ | 0.410 | 0 | 0 | [1] |
| $H_S$ | OH surface | 0.425 | 0 | 0 | [1] |
| $H_B$ | OH bulk | 0.425 | 0 | 0 | [1] |
| O | $H_2O$ | -0.820 | 0.31655 | 0.65019 | [1] |
| O | O bulk | -1.050 | 0.31655 | 0.65019 | [1] |
| $O_S$ | OH surface | -0.950 | 0.31655 | 0.65019 | [1] |
| $O_B$ | OH bulk | -0.950 | 0.31655 | 0.65019 | [1] |
| Fe | Fe bulk | 2.100 | 0.33020 | $7.7007\times10^{-6}$ | [2] |
| Bond [ß] | | $k^{ß}$ | b | | |
| O-H | $H_2O$ | 463700 | 0.100 | | [3-4] |
| O-H | OH | 327465 | 0.100 | | |
| Bend [γ] | | $k^{\square}$ | $\square^0$ | | |
| H-O-H | $H_2O$ | 383 | 109.47 | | [3-4] |
| Fe-$O_B$-H | Bulk | 251 | 109.47 | | [1] |

α. q is charge (e), σ□(nm) is the finite distance at which the inter-particle Lennard-Jones potential is zero and□ε (kJ/mol) is the Lennard-Jones potential well. Values of σ□(nm) from $R_o$ (Å) in CLAYFF ($V_{LJ}=\varepsilon((R_{o,ij}/r_{ij})^{1/12}-2(R_{o,ij}/r_{ij})^{1/6})$ were obtained as $\sigma\square R_o/10/2^{1/6}$. Those are from CHARMM-compatible.
ß. $k^b$ (kJ $mol^{-1}$ $nm^{-2}$) is the harmonic potential constant and b (nm) is the equilibrium bond length.
γ. $k^{\square}$ (kJ $mol^{-1}$ $rad^{-2}$) is the harmonic angle potential and $\square^0$ (deg) is the equilibrium angle.

**Table S5** Surface Fe-O bond lengths (nm) from MD

| Surface Species[α] | Crystallographic[5-6] | MD | |
|---|---|---|---|
| -O | 0.193 | 0.198 | (110) G |
| | 0.211 / 0.196 | 0.196 | (021) G |
| | 0.198 | 0.195 | (001) L |
| μ-O | 0.196, 0.196 | 0.200 | (110) G |
| | 0.193,0.196 / 0.210,0.211 | 0.198 | (021) G |
| | 0.199, 0.199 | 0.202 | (010) L |
| | 0.199, 0.199 | 0.198 | (001) L |
| $\mu_3$-O | 0.193, 0.196, 0.196 ($\mu_3$-O) | 0.196 | (110) G |
| | 0.211, 0.211, 0.210 ($\mu_{3,I,II}$-OH) | 0.210 | (110) G |
| | 0.207, 0.207, 0.198 | 0.206 | (001) L |

[α]Surface species were labeled in detail in Fig.2

**Table S6** MCR Analysis Results of ATR-FTIR spectra (Fig. 4)

| Components | | Band positions ($cm^{-1}$) | | | | Dominant spectra |
|---|---|---|---|---|---|---|
| LL | AI | 3667 | 3625 | 3552 | 3534 | Aa (-13.86)[α] - Ae (18.17) |
| | AII | 3645 | 3625 | 3552 | 3534 | Af (36.11) - Ai (312.99) |
| RL | BI | 3667 | 3626 | 3550 | 3534 | Ba (-7.85) - Be (0.24) |
| | BII | 3654 | 3626 | 3550 | 3534 | Bf (2.23) - Bk (35.67) |
| | BIII | 3646 | ▢ | 3550 | 3534 | Bl (69.44) - Bm (141.13) |
| G | CI | 3661 | 3648 | ▢ | 3491 | Ca (-12.00) - Ce (0.48) |
| | CII | 3658 | 3648 | 3545 | ▢ | Cf (1.18) - Ci (9.11) |
| | CIII | ▢ | 3648 | 3576 | ▢ | Cj (12.18) - Cl (17.88) |
| | CIV | ▢ | ▢ | 3585 | ▢ | Cm (20.46) - Cp (217.04) |

α. Numbers in brackets were proton concentrations in unit of protons per $nm^2$.

# FIGURES

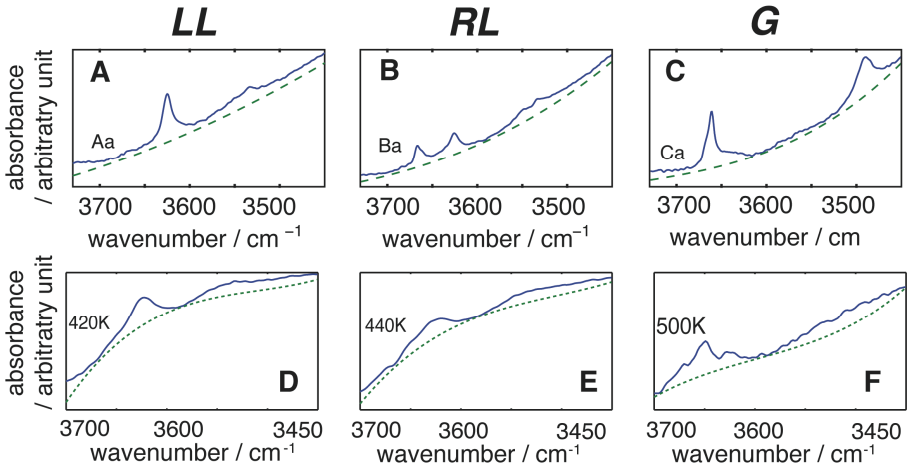


**Fig. S1** Background subtraction of ATR-FTIR and TPD spectra of evaporated different structures of FeOOH: LL (left column), RL (middle column) and G (right column). The original most alkaline spectra of synthetic LL, RL and G with each polynomial background (dash line) are plot in **A**, **B** and **C**. The spectra of highest temperature with each polynomial (dash line) are plot in **D**, **E** and **F**.

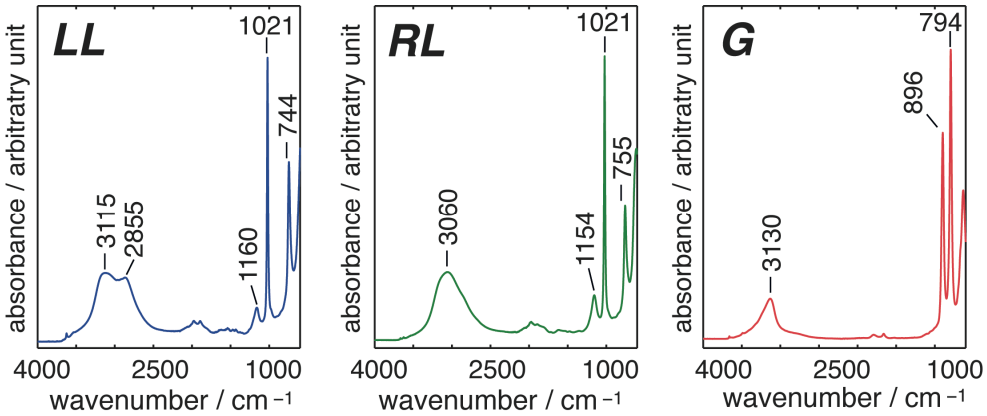


**Fig. S2** ATR-FTIR spectrum of dry dialyzed LL, RL and G. No other phases can be detected.

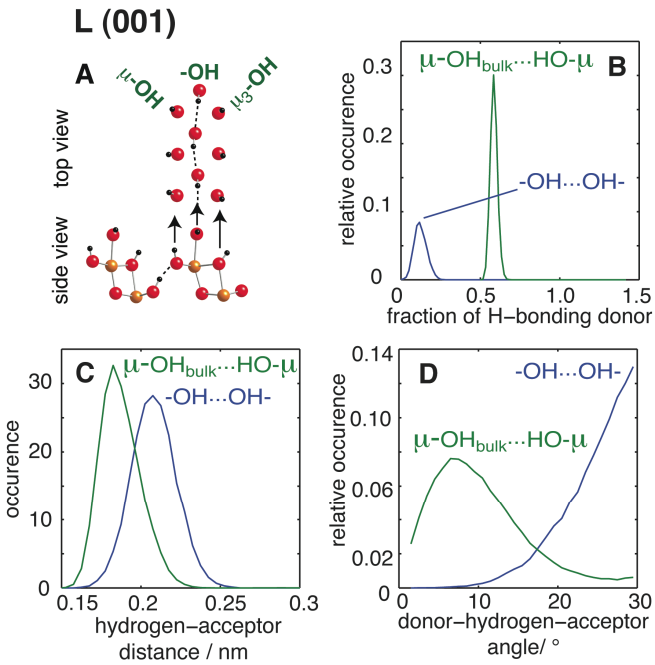


**Fig. S3** Molecular structure of (001) plane of lepidocrocite (**A**, Fe=yellow; O=red; H=black) and hydrogen bond analyzes of 5 ns MD simulations (**B-D**). The (010) plane of lepidocrocite (not shown) has only isolated hydroxyl groups.

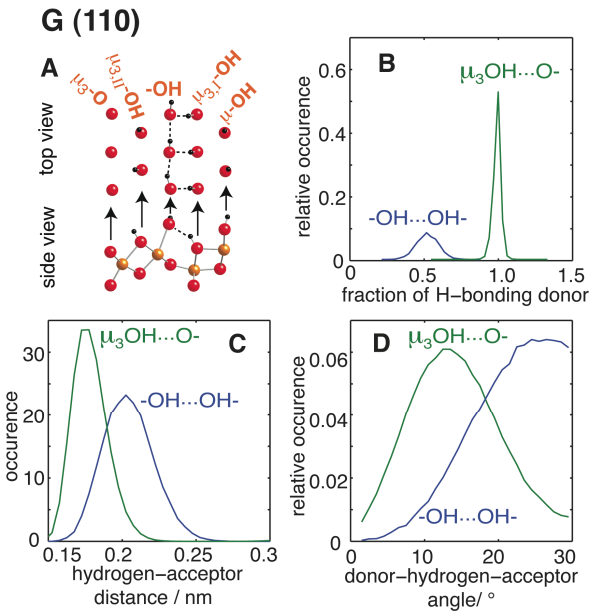


**Fig. S4** Molecular structure of (110) plane of goethite (**A**, Fe=yellow; O=red; H=black) and hydrogen bond analyzes of 5 ns MD simulations (**B-D**).

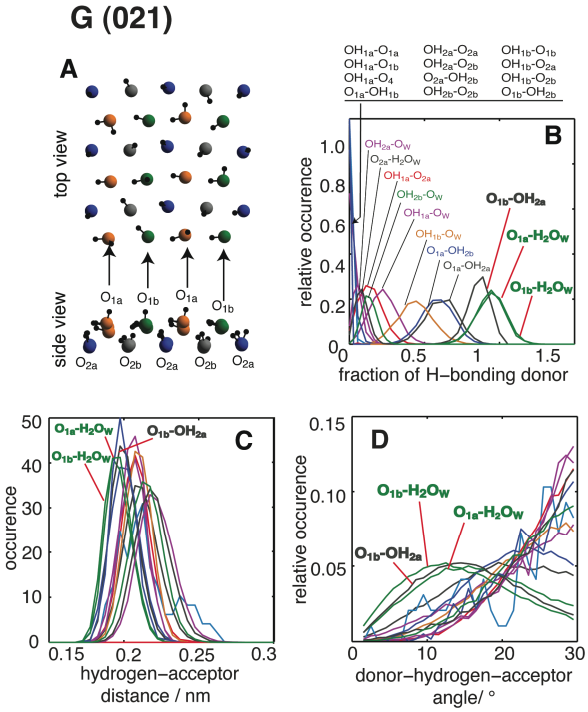


**Fig. S5** Site distribution (**A**) (O= blue&grey for two types of μ-OH; yellow&green for two types of -OH; H=black) and hydrogen bond analyzes of 5 ns MD simulations (**B-D**) of (021) plane of G. The strongest hydrogen bonds (highlighted in **B-D**) most likely occur between one class of μ-OH sites (labeled a -$OH_{2a}$) and -OH ($O_{1b}$), as well as all -OH sites with chemisorbed water (labeled with subscript "w").

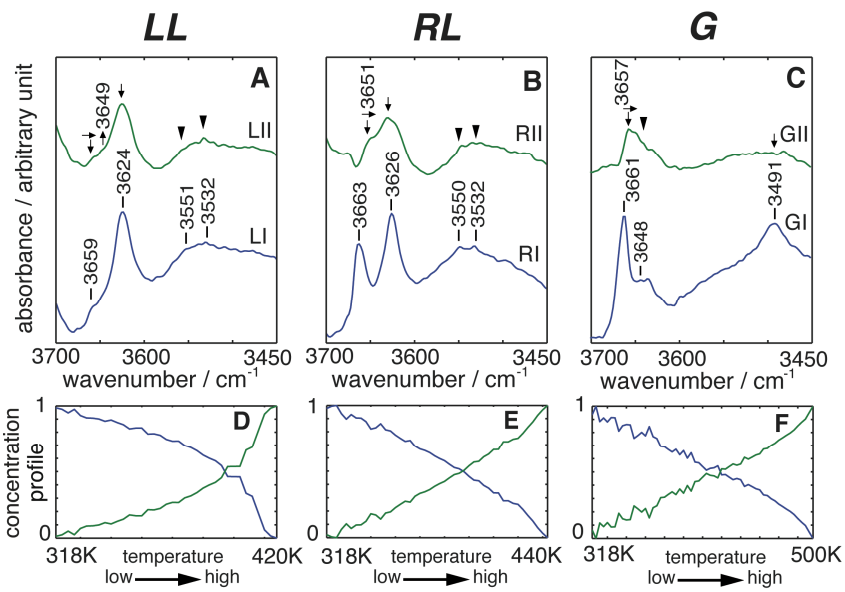

**Fig. S6** MCR spectral components of LL (**A**), RL (**B**) and G (**C**) obtained from spectra of TPD experiments (Fig. 5). Corresponding concentration profiles are shown in **D-F**.